CODEN [USA]: IAJPBB ISSN : 2349-7750

INDO AMERICAN JOURNAL OF
PHARMACEUTICAL SCIENCES
SJIF Impact Factor: 7.187

Available online at: http://www.iajps.com *Research Article*

FORMULATION AND EVALUATION OF HMG-CoA REDUCTASE INHIBITOR NANOPARTICLES

Y. Ramulu
Assistant Professor, Department of Pharmaceutics, Sree Dattha Institute Of Pharmacy, Sheriguda, Hyderabad, Telangana, India.

Article Received: January 2023 **Accepted:** January 2023 **Published:** February 2023

Abstract:
The present work was proposed to prepared nanoparticles loaded with Rosuvastatin to achieved better bioavailability with low dose of the drug at the site, decreased the risk of adverse side effects. Rosuvastatin nanoparticles were prepared by in-situ two step desolvation method. The loading efficiency(F1) and Entrapment efficiency(F1) was 66.21 and 91.73 respectively. The shape of nanoparticle was found to be spherical by SEM analysis. Formulation with high polymer content was observed to be fairly spherical. Compatability of drug and polymer mixture was done by performing FTIR and DSC study. It was concluded that there was no interaction between drug and polymer. The in-vitro released of Rosuvastatin was evaluated in phosphate buffer saline (pH6.8) up to 16hrs. The formulation F1 was released the drug 93.38% up to16 hours. and chosen the best among the formulations were prepared. Zeta potential was determined for the formulation F1 and it was found to be +ve value of 1.57mv. The in-vitro drug released data was applied to various kinetic models like zero order kinetics, Higuchi plot, first order kinetics, and Peppas plot by predict the drug release kinetics mechanism. The formulation F1 was best fitted the zero order kinetics. In short term stability studies the formulation F1 was showed that there was no remarkable changes in the % drug loading efficiency. Based on the % drug loading efficiency, zeta potential, in-vitro drug release profile, in-vitro drug release kinetics and stability studies the formulation F1 was found to be best one among the formulations (F1 to F8) were prepared. These nanoparticles can be promising agents for rational drug delivery in lipidemic condition.

Keywords: *Formulation, Characterization, Rosuvastatin, Nanoparticles*

Corresponding author:
Y. Ramulu,
Assistant Professor,
Department of pharmaceutics,
Sree dattha institute of pharmacy,
Sheriguda, Hyderabad, Telangana.
India. E-mail: ramupharma846@gmail.com

QR code

Please cite this article in press Y. Ramulu. ***Formulation And Evaluation of HMG-CoA Reductase Inhibitor Nanoparticles****., Indo Am. J. P. Sci, 2023; 10 (02).*

INTRODUCTION:

In the last 50 years, material researchers have been extensively studying how to exploit nanoparticles and nanostructured materials in different biomedical and healthcare sectors [1]. The term "NP" usually defines minute particles of matter (1 to 100 nm in diameter), but other names can be used to describe larger particles (up to 500 nm in diameter). For example, nanorods, nanowires, and nanofibers are nanoparticles with a diameter in the 1–100 nm range but with one dimension outside the nanoscale dimension [2]. Nanostructured materials are nanomaterials with one dimension in the nanoscale range (<100 nm) and are made of a single material or multiple materials. Therefore, nanostructured materials are composed of interlinked parts in the nanoscale range [3]. Nanoparticles and nanostructured materials can be made of simple materials (e.g., metal, carbon, polymer) [4], of composites (e.g., polymer-metal, silica-metal, graphene-metal), or in the core-shell form [5,6,7,8]. Nanomaterials are typically synthesized by one of two main approaches, i.e., bottom-up approach and top-down approach. Among all the methods, recently, the synthesis of nanomaterials by physical vapor deposition, chemical vapor deposition, electrospinning, 3D printing, biological synthesis, and supercritical fluid have gained importance, which is mingled with other methods to improve the synthesis efficiency [9,10]. Nanomaterials display many interesting features, such as superior mechanical performance, the possibility of surface functionalization, large surface area, and tunable porosity, compared to their bulk materials [11,12,13]. These outstanding features explain why nanomaterials are the perfect candidates in the biomedical sector for the production of tissue-engineered scaffolds (e.g., blood vessels, bone), drug delivery systems (gene therapy, cancer treatments, drugs for chronic respiratory infections), chemical sensors [4,5], biosensors [6,7], and wound dressings [14,15]. Remarkably, several studies suggest that ancient civilizations in India, Egypt, and China used nanotechnology (metallic gold) for therapeutic purposes in 2500 BC [16]. Nanomaterials' discrete features can complicate the assessment of the effects and the toxicity risk associated with their use in a biological environment. Indeed, nanomaterials' chemical composition, size, shape, surface charge, area, and entry route in the body can influence their biological activities and effects [17]. In bioimaging, tailored fluorescent nanoparticles could outperform traditional molecular probes as fluorescent indicators, particularly in terms of sensitivity [18]. Tissue-engineered nanofiber scaffolds are considered the best option to manage tissue loss and end-stage organ failure and have already helped millions of patients worldwide [15]. Three-dimensional nanofibrous scaffolds are polymer-based structures with balanced moisture, absorption, strongly organized porosity (60–90%), and gas permeability, comparable to native extracellular matrices [15]. One and two-dimensional nanomaterials can be used for signal amplification, are nanosized (≤100 nm), have high electrical conductivity, and are compatible with drugs [13] and biological molecules [12]. They have also been used for the early detection of diseases (e.g., virus, bacterial, cancer). Antimicrobial nanomaterials (e.g., Ag, Au, CuO NPs) are frequently employed in dermatology because they contribute to accelerating wound healing and preventing/treating bacterial infections [19,20]. Based on dimensionality, nanomaterials are classified mainly into four groups [1]: 0D, where length, height, and width are fixed at a single point; 1D, where only one parameter exists (e.g., carbon nanotubes); 2D, where length and width exist (e.g., graphene); and 3D, where length, height, and width exist [21]. For example, a graphene nanosheet is a typical example of a 2D nanostructure with a thickness in the nanoscale range. Theoretically, single-layer graphene is 0.345 nm thick (one atom thickness) and up to 500 nm in diameter. Based on their chemical composition, nanoparticles and nanostructured materials can be categorized into four types: organic nanomaterials (e.g., micelles, dendrimers, polymersomes, hydrogels, nanoconjugates), inorganic nanomaterials (e.g., metals, metal oxide, and ceramic nanomaterials), carbon-based nanomaterials (fullerenes, carbon nanofibers, diamonds carbon nanotubes, and graphene), and composite nanostructures [1,22]. The synthesis of traditional nanosized products contributes to the present and future economic growth of many countries. Based on porosity, nanomaterials can be classified into porous and non-porous materials [3]. Porous materials have a less dense molecular structure to allow airflow or the absorption of atoms, ions, and molecules. Non-porous materials are denser, do not absorb well, and allow limited airflow. Mesoporous (or super-nanoporous) nanomaterials are nanoporous materials with pores of 2–50 nm in diameter [23,24]. Recent research has focused on mesoporous nanomaterials for delivering therapeutic agents to tumor cells with little drug leakage into healthy cells. The high porosity, surface functionality, and small pore size of mesoporous nanoparticles allow the controlled release and efficient drug loading at the target site [22].

Application of nanotechnology in drug delivery system has opened up new areas of research in controlled release of drugs. The nanoparticle represents promising drug delivery system of

controlled and targeted drug release which shows and maintains the therapeutic concentration forlong period of time. The reported bio- availability of Rosuvastain is less. Hence the present study was undertaken to develop the bioavailability of the drug. While forming the nanoparticleformulation it increased the absorption and bio- availability. The present work of nanoparticles are focused on Rosuvastatin loaded gelatin nanoparticle by two step desolvation method. Hence the novel delivery system applied to antilipidemic drugs. Some biodegradable carriers degrade in the body. This problem is overcome in this nanoparticle's carriers. In long term therapy fluctuations in the plasma concentrations, with high concentration peaks are common for drugs with rapid absorption and elimination. Such characteristic makes Rosuvastatin is a suitable candidate for to prepare desired nanoparticulate drug delivery system. Rosuvastatin is the widely used category of anti lipedimic drug in the treatment of high cholesterol condition. The aim of present work was to formulate by using polymer like gelatin A and Gelatin B nanoparticles containing Rosuvastatin in order to provide therapeutic effect.

MATERIALS AND METHODS:

MATERIALS: Rosuvastatin procured from Torrent pharmaceuticals Ltd, Ahmedabad. Gelatin – A, Gelatin – B, Glutaraldehyde 25%, Sodium sulfate, Sodium metabisulfite purchased from S.D fine-chem limited, Mumbai.

METHODS:

Preformulation studies

Preformulation testing was an investigation of physical and chemical properties of a drugsubstance alone. It was the first step in rational development of dosage form.

Analytical methods

Determination of λ max

The absorption maximum of the standard solution was scanned between 200-400 nm regions onUV-VISIBLE spectrophotometer. The absorption maximum obtained with the substance being examined corresponds in position and relative intensity to those in the reference spectrum

Development of standard curve of Rosuvastatin in methanol: (*Alka Gupta., et al., 2005)*

25 mg of Rosuvastatin Calcium was weighed accurately and transferred into 50 ml volumetric flask and dissolved in Methanol, after dissolution the volume was made up to the mark with Methanol (500mg/ ml). Further dilution was made by pipetting 1 ml of mother liquorinto 50 ml s to acquire 10 mg/ ml solution made up with methanol. The absorbance measurements of these solutions were carried out against methanol as blank at 244 nm. A calibration curve of Rosuvastatin was plotted.

Preparation of methanol solution*(IP, 2007)*

Methanol was prepared according to I.P. 2007.

Preparation of stock solution of Rosuvastatin in methanol:

Accurately weighed 100 mg of Rosuvastatin was dissolved in little quantity of 100ml of methanol and 1ml of solution was taken & make up to 10ml (100µg/ml) volume was the same to prepared standard solution having concentration of 100 µg/ ml.

Procedure:

From the stock solution, aliquots of 1, 2, 3, 4, 5,6 and 7 ml were transferred to 10 ml volumetric flasks and final volume was made to 100ml with methanol. Absorbance values of these solutions were measured against blank (methanol) at 244 nm using uv-visible spectrophotometer

Development of standard curve of Rosuvastatin in 6.8 phosphate buffer:*(IP, 2007)*

Preparation of 6.8 phosphate buffer:

Place the 50 ml of 0.2M potassium dihydrogen phosphate in a 200 ml of volumetric flask.And add specified volume of 0.2 M sodium hydroxide then add water to volume torequired.

Preparation of 0.2 M sodium hydroxide:

Dissolve the sodium hydroxide in water to produce 40 to 60 %w/v solution and allow to stand and finally add 8 gm of sodium hydroxide in 1000 ml.

Preparation of 0.2 M potassium dihydrogen phosphate:

Dissolve the 27.218 gm of potassium dihydrogen phosphate in water to dilute with water 1000ml.

Preparation of stock solution of Rosuvastatin in 6.8 phosphate buffer:

Accurately weighed 100 mg of Rosuvastatin was dissolved in little quantity of 100ml of

6.8 phosphate buffer and 1ml of solution was taken & make up to 10ml (100µg/ml) volume wasthe same to prepared standard solution having concentration of 100 µg/ ml.

Procedure: From the stock solution, aliquots of 1, 2, 3, 4, 5,6 and 7 ml were transferred to 10 ml volumetric flasks and final volume was made to 100ml with methanol. Absorbance values of these solutions were measured against blank (6.8 phosphate buffer) at 240 nm using uv-visible spectrophotometer

Determination of percentage purity of drug *(Dhirendra K., et al., 2010; IP, 2007)*

Standard solution Preparation:
Standard solution of Rosuvastatin calcium was prepared by dissolving 10mg of Rosuvastatin calcium in 100ml of methanol. To obtained the concentration 100µg/ml. Further diluted 5-50ml by same solvent to obtained a solution containing 10µg/ml.

Sample solution preparation:
Pure raw materials of Rosuvastatin calcium were weighed and powdered. Amount of powdered equivalent to 20 mg taken into a 200ml volumetric flask, 140 ml methanol added to dissolve the drug, cooled the flask up to the room temperature and methanol was added to make up the volume up to the mark,Centrifuged at 4000 rpm for 10mins, further diluted 5ml to 50ml with same solvent to obtain a solution containing 10 µg/ml. Same procedure was used for two other market samples of Rosuvastatin calcium.

Preparation of Nanoparticles (*Ze Lu et al.,2004)*
The nanoparticles were prepared by *in-situ* nano emulsion polymer Two step desolvation method, by using a different drug and polymer ratios. The formulations were designated as F-1, F-2, F-3, F-4, F-5, F-6, F-7 and F-8respectively.
The compositions of formulations

S.NO	Formulations							
	Gelatin A ratio				Gelatin B ratio			
Ingredients (gm)	F1 (1:1)	F2 (1:2)	F3 (1:3)	F4 (1:4)	F5 (1:1)	F6 (1:2)	F7 (1:3)	F8 (1:4)
Rosuvastatin	1	1	1	1	1	1	1	1
Gelatin A	1	2	3	4	-	-	-	-
Gelatin B	-	-	-	-	1	2	3	4
Sodium sulphate (20%) ml	2	2	2	2	2	2	2	2
Sodium megabisulphate (12%) ml	5	5	5	5	5	5	5	5

Two step desolvation method:
Gelatin (200 mg) was dissolved in 10 ml of water containing of 2% Tween 20. The solution was heated at 40°C with constant stirring at 300 rpm. To this solution, 2 ml of a 20% aqueous solution of sodium sulfate was added slowly, followed by 1 of isopropanolcontaining2 mg of Rosuvastatin. A remaining of sodium sulfate solution (5.5–6 ml) was addeduntil the solution turned turbid, (which indicated the formation of gelatin aggregates.) Approximately 1 ml of distilled water was then added until the solution turned clear. An aqueoussolution of glutaraldehyde [25%, (0.4 ml)] was added to cross-link with the gelatin. Sodium metabisulfite solution [12%, (5 ml)] was added after 5 minutes to stop the cross-linking process. After 1 hour, the crude product was purified on a Sephadex G-50 column. The nanoparticle containing fraction was lyophilized in a freeze drier over a 48 hour period.

RESULTS:

Preformulation parametersIdentification of drug

Identification by FTIR spectroscopy
The FTIR spectrum of Rosuvastatin was shown in Figure 1 and the interpretations ofFTIR frequencies were showed in Table 1

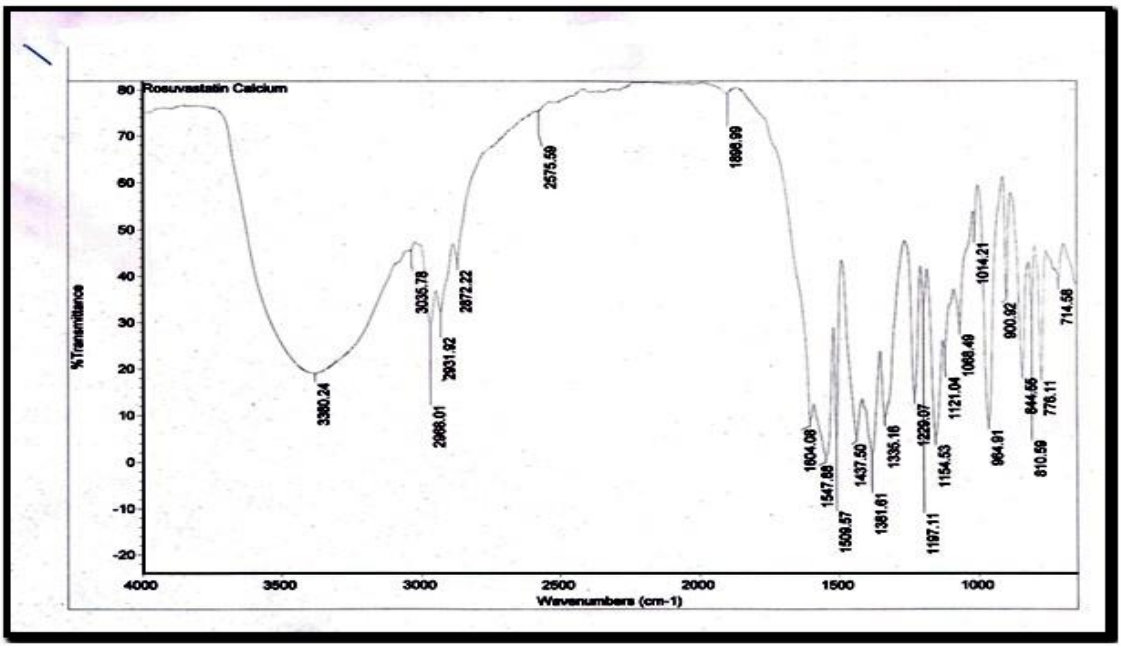

Figure 1:FTIR spectrum of Rosuvastatin

Table 1: Characteristic frequencies in FTIR spectrum of Rosuvastatin

Wave no.(cm^{-1})	**Inference**
1335	So_2 stretching
1068	C-F stretching
1381	C-N stretching (aromatic amine)
3035	C-H stretching
1604	C=C Skeletal stretching (Aromatic)
2968	C-H stretching
2872	CH_3 symmetric stretching
3380	C-H stretching
1728	C=O stretching
1547	CO_2 symmetric stretching
810	C-S stretching

Interpretation of FTIR Spectrum

Major functional groups like Aliphatic Ethers,Aliphatic Hydrocarbons, and Primary Aliphatic Alcohols,present in Rosuvastatin showed characteristic peaks in FTIR spectrum. The majorpeaks were identical to functional group of Rosuvastatin. Hence, the sample was confirmed as Rosuvastatin

Melting point

Melting point values of Rosuvastatin sample was found to be in range of 155^0C to 156^0C.The reported melting point for Rosuvastatin was154.33^0C. Hence, experimental values were fitted with standard values.

Physicochemical parameters of drugOrganoleptic properties
Odour: Odourless
Colour: White or almost white
Nature: Crystalline powder.
Loss on drying
The percentage loss on drying after 3 hours was found to be as follows

Table 2: Percentage loss on drying for Rosuvastatin

S. No	Percentage LOD	Avg. percentage LOD
1	0.7	0.5666±0.25
2	0.4	
3	0.8	

The sample passes test for loss on drying as per the limit specified in IP, 2007 (N.M.T. 1%).Itwas shown in Table 2

Analytical methods
Determination of λ max in 0.1N methanol:
The absorption maximum for Rosuvastatin in 0.1N Methanol was found to be 244 nmand absorption maximum was shown in Figure 2.

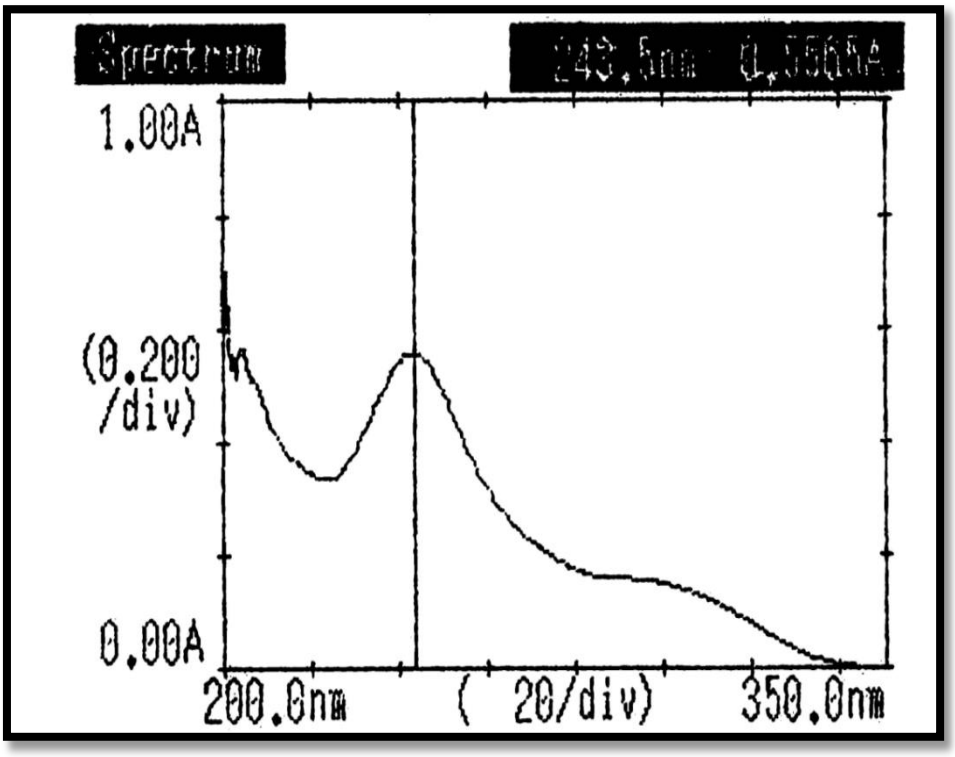

Figure 2: λ max observed for Rosuvastatin in 0.1N Methanol

Preparation of standard graph of Rosuvastatin in 0.1N methanol
Absorbance obtained for various concentrations of Rosuvastatinin 0.1N Methanol were given in Table.3 and Figure 3. The graph of absorbance vs concentration for Rosuvastatin wasfound to be linear in the concentration range of 10 µg /ml. The calibration curve parameters shown in Table.4 So the drug obeys Beer- Lambert's law in the range of 10 µg /ml.

Table 3 : Data of concentration and absorbance for Rosuvastatin in 0.1N Methanol

S.NO	Concentration(µg/ml)	Absorbanceat 244nm
1	0	0
2	1	0.062
3	2	0.122
4	3	0.183
5	4	0.245
6	5	0.308
7	6	0.371

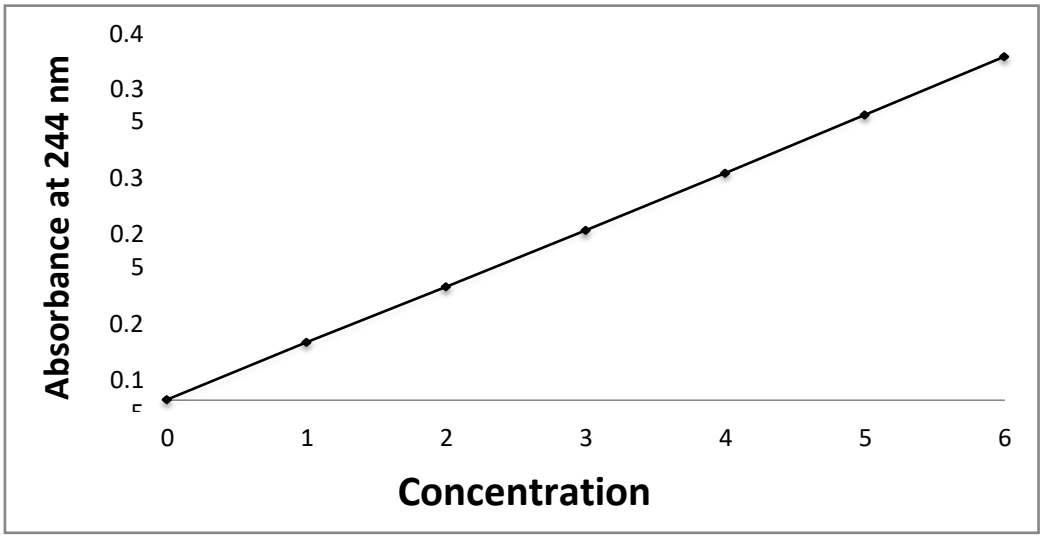

Figure 3: Calibration curve of Rosuvastatin calcium in methanol at 244 nm

Table 4: Data for calibration curve Parameters for 0.1 methanol

S.NO	PARAMETERS	VALUES
1	Correlation coefficient (r^2)	0.99996
2	Slope (m)	0.06171
3	Intercept(c)	-0.00071

Determination of λ max in 6.8 phosphate buffer:

The absorption maximum for Rosuvastatin in 6.8 phosphate buffer was found to be240 nm and absorption maximum was shown in Figure 4

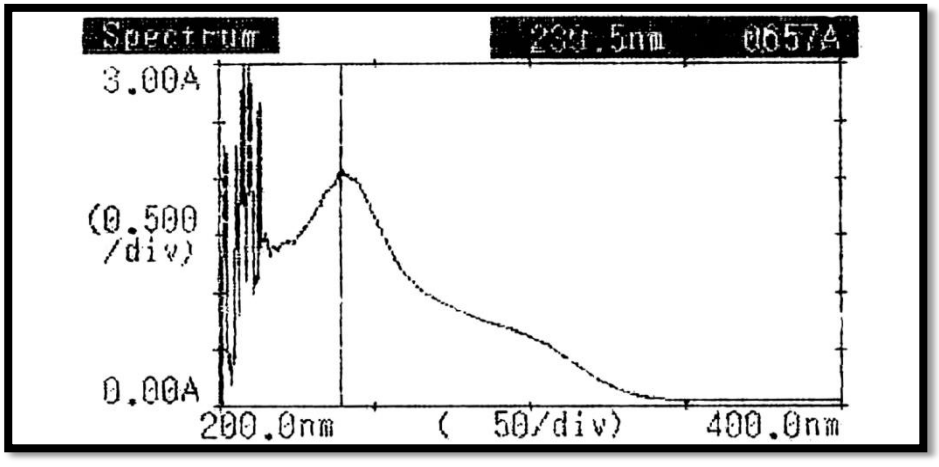

Figure 4: λ max observed for Rosuvastatin in 6.8 buffer

Preparation of standard graph of Rosuvastatin in 6.8 phosphate buffer:
Absorbance obtained for various concentrations of Rosuvastatin in6.8 phosphate buffer were given in Table 5.and Figure 5 .The graph of absorbance vs concentration for Rosuvastatin was found to be linear in the concentration range of 10 µg /ml.The calibration curveparameters shown in Table 6.So the drug obeys Beer- Lambert's law in the range of 10 µg /ml.

Table 5: Calibration curve of Rosuvastatin calcium in 6.8 phosphate buffer at 240 nm

S.NO	Concentration (µg/ml)	Absorbance at 240nm
1	0	0
2	1	0.071
3	2	0.142
4	3	0.211
5	4	0.278
6	5	0.349
7	6	0.423

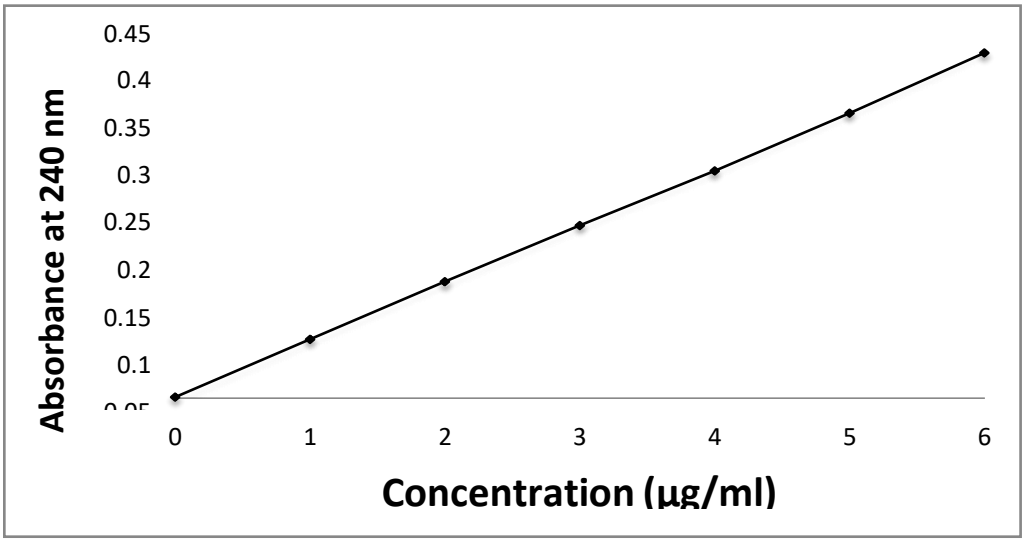

Figure 5: Calibration curve of Rosuvastatin calcium in 6.8 buffer at 240 nm

Table 6 : Data for calibration curve Parameters for in 6.8 phosphate buffer

S.NO	Parameters	Values
1	Correlation coefficient (r^2)	0.999936
2	Slope (m)	0.0070036
3	Intercept (c)	-0.000464

Percentage purity of drug
The percentage purity of drug was calculated by using calibration graph method (leastsquare method).

Table 7: Percentage purity of drug

S. No	Percentage purity (%)	Average percentage purity (%)
1	99.10	99.07±1.24
2	99.53	
3	99.60	

All the values are expressed as mean± S.D., n=3.

The reported percentage purity for Rosuvastatin in IP 2007 is 98 to 99.53%.

Interpretation of FTIR spectrum:

Table 8: Interpretation of FTIR spectrum

S.NO	FORMULATION	WAVE NUMBER (CM^{-1})
1.	Pure Rosuvastatin	3380.24,3055.78,2968.01,2931.92,2872.22,2575.59,1898.99 1604.08,1547.88,1509.57,1437.50,1381.61,1335.16,1229.07,1197.11, 1154.53,1121.04,1068.49,1014.21,964.91,900.92,844.55,810.59,776.11, 714.58
2.	Gelatin	2959.12,2926.12,2855.03,2644.11,2400.33,2140.11,1981.23,1731.97,168 5.40,1630.59,1562.14,1510.10,1451.12,1406.01,1326.57,1245.14,1192.35 ,1156.55,1180.31,1022.55,970.48,918.44,871.87,773.26,721.22,668.20
3.	Rosuvastatin+ Gelatin	3378.20,2968.34,2934.43,2872.44,2572.85,2501.63,2438.62,2095.31,190 7.21,1608.63,1554.73,1444.27,1380.42,1334.82,1229.07,1197.20,1154.08 ,111.30,1068.58,1014.82,965.00,900.91,810.68,844.62,776.15,714.62

The major peaks observed in drug spectrumalso observed in drug with polymerspectrum. Therefore FTIR spectrums were compared; it could indicate that there was no incompatibility between drug and polymer.

By DSC thermal analysis

The compatibility and interactions between drugs and polymer were analysedbyDSCthermogram and results were obtained represented and shown in Figure 6 to 8

Figure 6: DSC thermo grams of Rosuvastatin

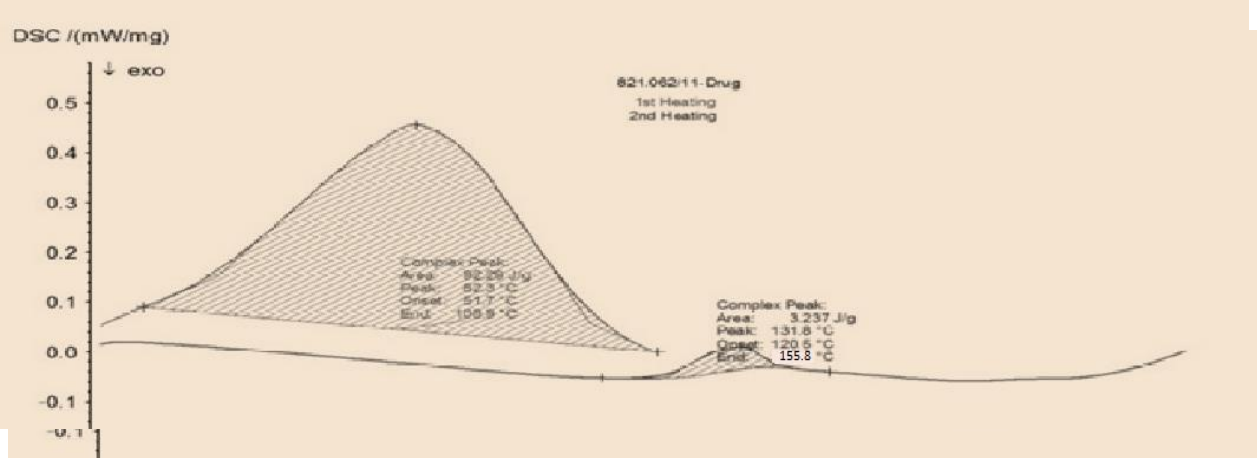

Figure 7:DSC thermo grams of Rosuvastatin+ gelatin A

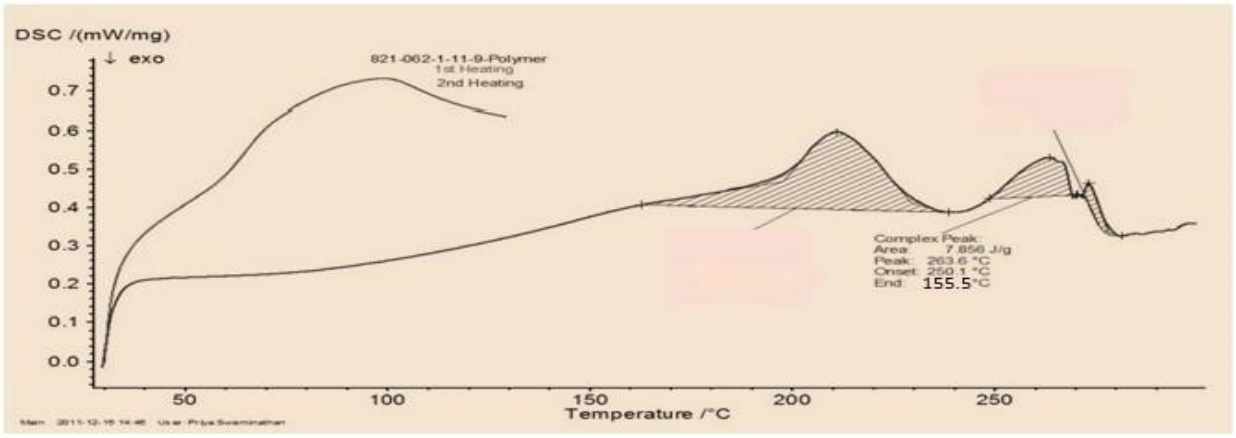

Figure 8:DSC thermo grams of Rosuvastatin+ gelatin B

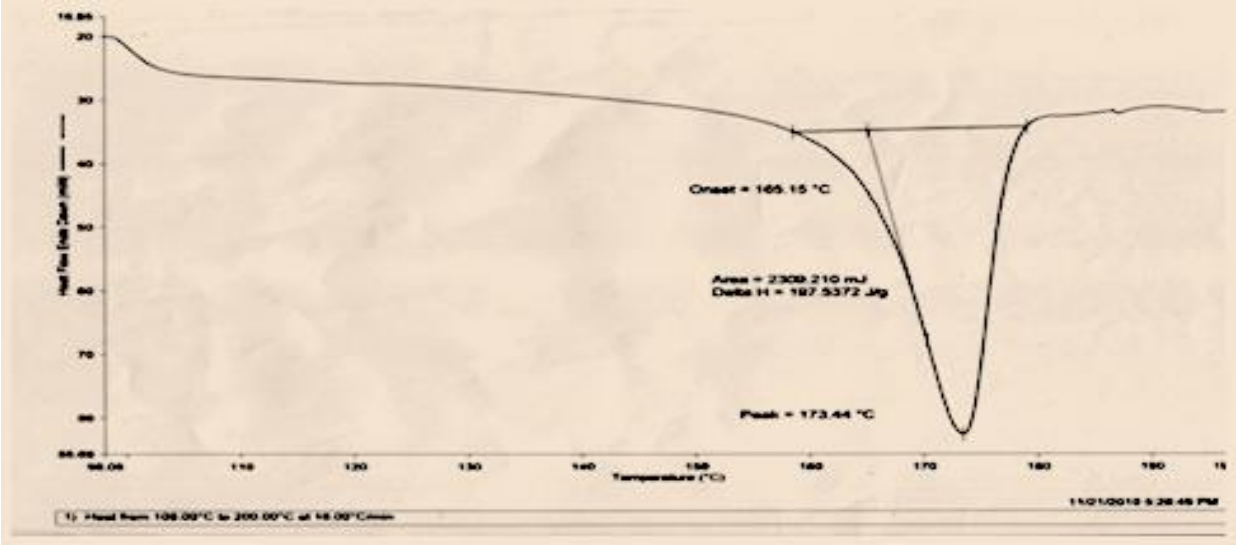

The possible drug and polymer interaction can be studied by using DSC. The Rosuvastatinexhibits a sharp endometric peak 155.8 which is corresponding with its melting point at figure 7 and the Rosuvastatin + gelatin A and B exhibits the sharp endometric peak 155.5 at figure 8. Therefore when compared with pure drug thermo gram. No interaction was found betweendrug and polymers.

Characterization of nanoparticles

Drug loading efficiency (%le) and drug loading capacity (%LC):

The results were shown in Table 9 and Figure.9. It is revealed that the highest, %LE and %LC in the nanoparticle preparation were obtained.

Table 9: % LE and % LC of Rosuvastatin nanoparticles with gelatin A and gelatin B

S.NO	Parameter	Formulation (Gelatin A)				Formulation (Gelatin B)			
		F1	F2	F3	F4	F5	F6	F7	F8
1	Drug entrapment efficiency (LE %)	91.73	72.93	76.50	86.27	69.85	87.74	88.68	68.72
2	Drug loading capacity (Lc %)	66.21	55.62	49.41	39.54	65.22	54.14	61.33	47.54

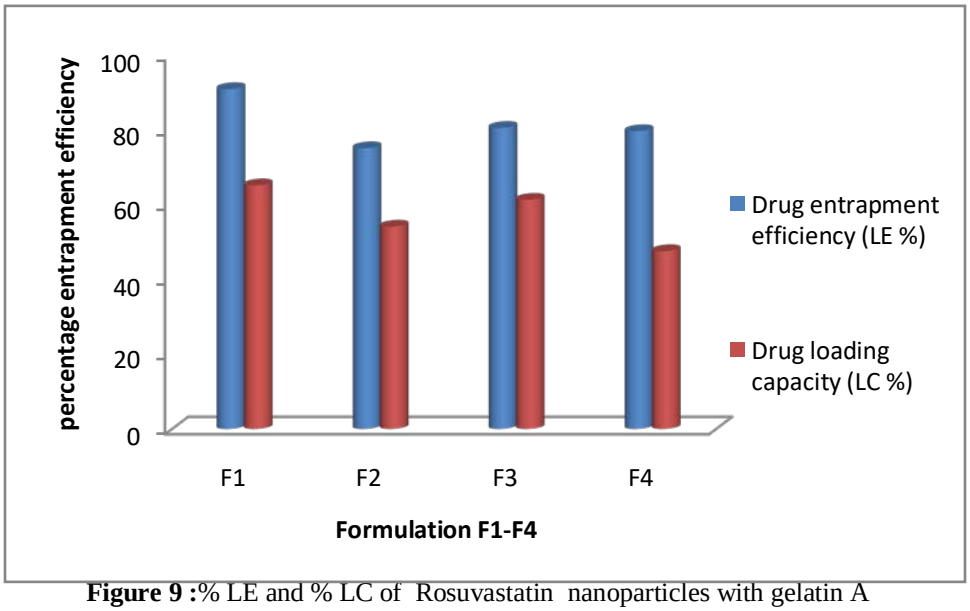

Figure 9 :% LE and % LC of Rosuvastatin nanoparticles with gelatin A

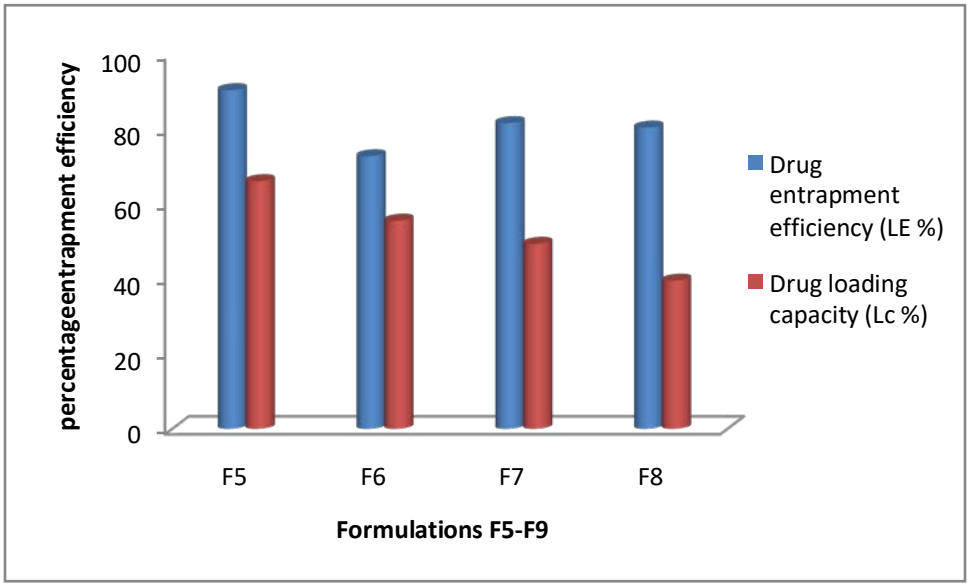

Figure 10:% LE and % LC of Rosuvastatin nanoparticles with gelatin B

Morphological characterization of F1 to F4 (gelatin A)

Rosuvastatin loaded polymeric nanoparticles were fabricated using*in-situ* two step desolvation method using polymer Gelatin A.

The choice of an *in-situ* two step desolvation method of encapsulation was usuallydetermined by the %yield, LE and %LC of the drug and sonication process which allowed reducing considerably the mean particle size and simultaneously to narrow the width of the size distribution, i.e. reduces the polydispersity index. The effectiveness of *in-situ* two step desolvation method and polymer on nanoparticle preparation was confirmed by their size, *in- vitro* release characteristics.

Morphological characterization of F5to F8 (gelatin B)

Rosuvastatin loaded polymeric nanoparticles were fabricated using*in-situ* two step desolvation method using polymer Gelatin B.

The choice of a of two step desolvation method encapsulation was usually determined by the solubility characteristics of the drug and high pressure homogenization process which allowed reducing considerably the mean particle size and simultaneously to narrow the width of the size distribution, i.e. reduced the polydispersity index. The effectiveness of two step desolvation method and polymer, on nanoparticle preparation was confirmed by their size,*in-vitro*release characteristics.

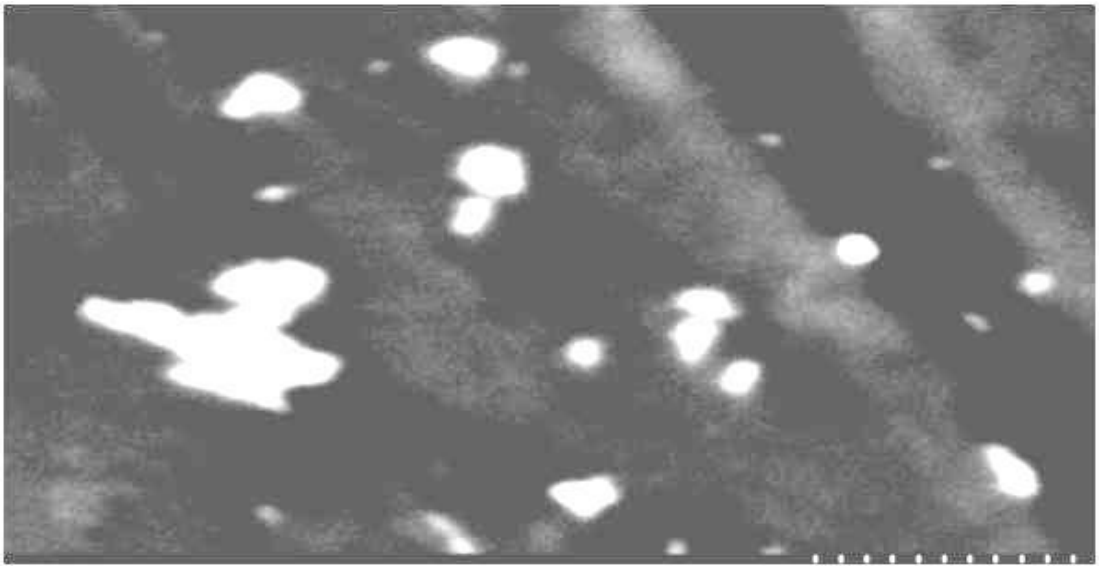

Figure 11: Scanning electron microscopy image of F1

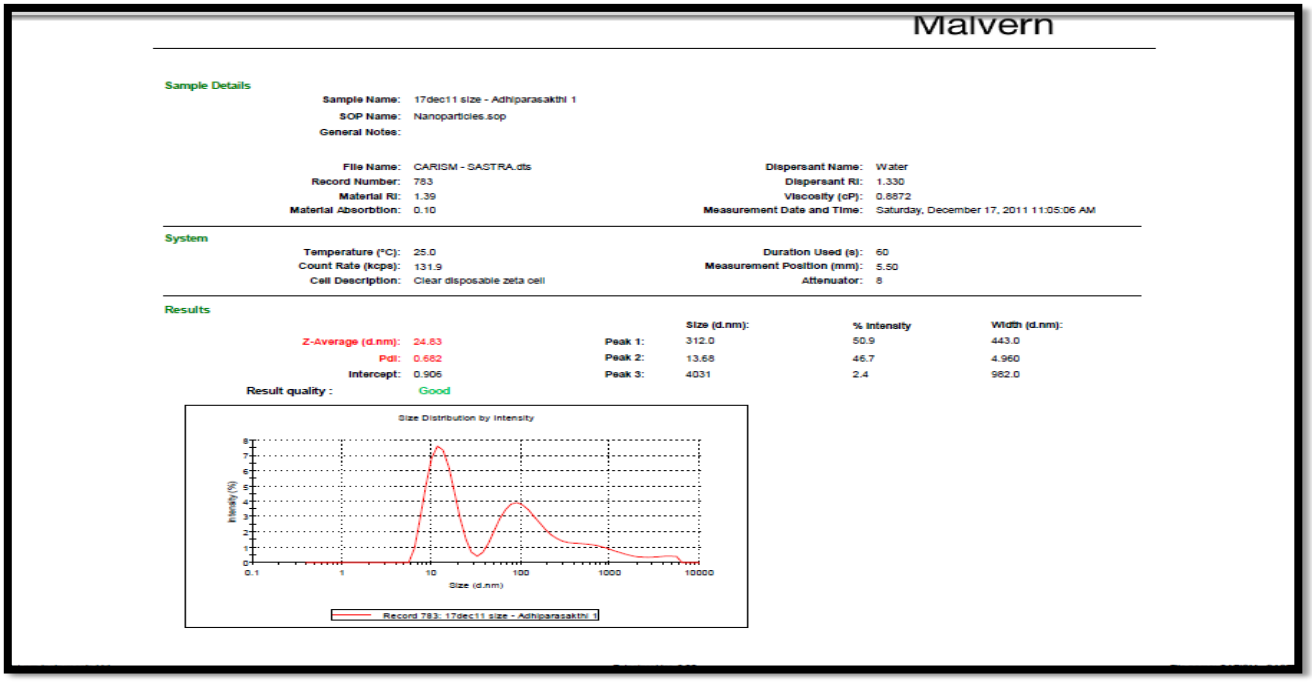

Figure 12: Particle size distribution F1

In-vitro Drug Release profile

In-vitro drugreleased profiles of Rosuvastatin nanoparticles were performed in eachformulation dipped in the phosphate buffer (6.8 pH) upto 16 hours. It was represented in Table 10

Table 10 Percentage in vitro drug released of Formulations F1-F8

S. No	Time in hours	pH medium	Gelatin A Percentage drug released(%)				Gelatin B Percentage drug released (%)			
			F1 %	F2 %	F3 %	F4 %	F5 %	F6 %	F7 %	F8 %
1	2	6.8 phosphate buffer	11.49± 0.11	12.83± 0.32	9.26±0. 37	10.60± 0.52	9.71±0. 65	7.48±1. 87	8.37±0. 25	13.50± 0.89
2	4		21.76± 0.22	20.86± 0.23	16.8±0. 25	16.62± 0.35	19.30± 0.44	15.95± 0,21	17.29± 0.87	22.87± 1.25
3	6		33.13± 0.52	32.46± 0.36	30.9±1. 25	30.01± 0.54	31.35± 0.87	28.45± 0.78	29.34± 0.54	31.39± 1.22
4	8		48.30± 0.17	43.84± 0.21	44.07± 0.36	44.96± 0.58	47.63± 1.58	45.85± 0.25	46.03± 0.77	45.40± 0.57
5	10		63.47± 0.33	61.02± 0.87	62.81± 0.14	61.98± 1.25	64.14± 0.47	62.14± 0.74	63.44± 0.52	63.92± 0.11
6	12		79.76± 0.54	78.20± 1.22	75.97± 0.87	74.41± 1.74	77.31± 1.87	76.41± 1.25	75.08± 1.58	75.97± 1.87
7	14		87.87± 0.58	85.56± 1.25	79.09± 0.65	81.99± 0.98	85.78± 1.22	84.89± 0.78	83.11± 1.32	82.66± 0.85
8	16		93.38± 1.20	92.25± 0.44	88.24± 1.47	84.89± 0.14	92.49± 0.57	91.59± 0.87	87.35± 0.58	86.68± 0.74

All the values were expressed as mean ± SD., n=6

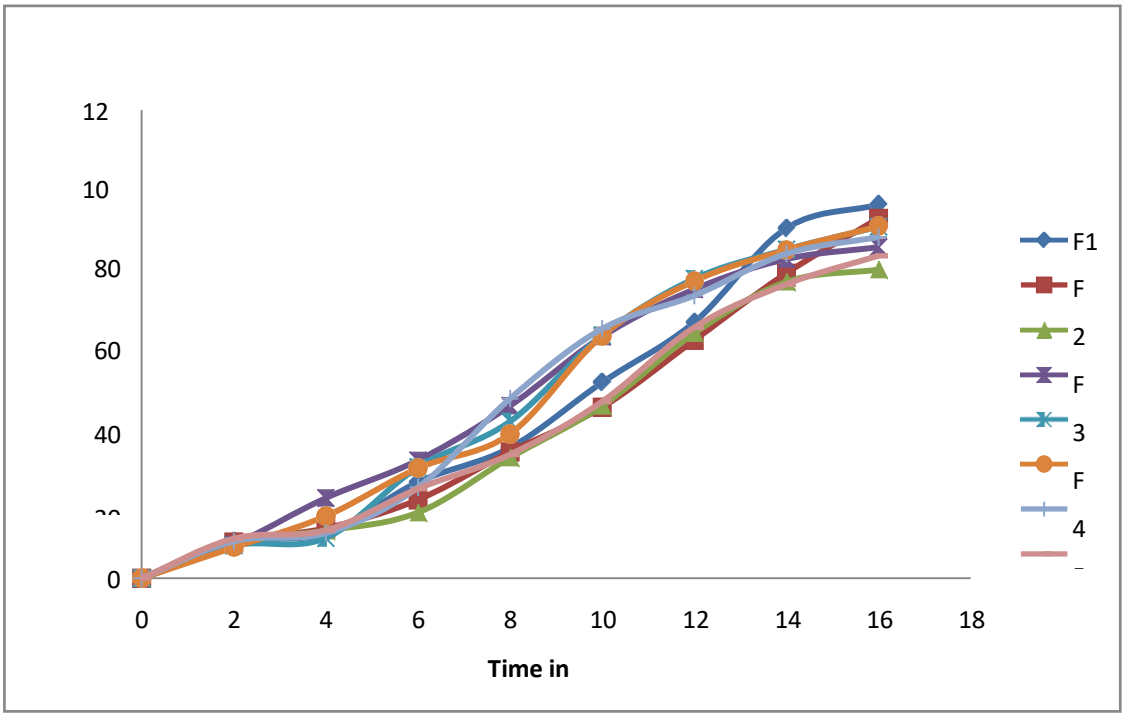

Figure 13: Graphical representation of comprehensive *invitro* percentage drug released for formulations F1-F8

Release Kinetics of *In-vitro* Drug Release

The kinetics of *in-vitro* drug released was determined by applying the drug release datato various kinetic models such as zero order first order, Higuchi and Korsmeyer- Peppas. The results obtained were represented Table 11 and Figure 8.25 to 8.32.

Table 11: Release kinetics of *In-vitro* drug release gelatin A and gelatin B

Formulations	Zero order R^2	First order R^2	Higuch R^2	Peppas R^2	Best Fit Model
F1	0.991	0.845	0.978	0.837	Zero
F2	0.986	0.873	0.974	0.734	Zero
F3	0.983	0.914	0.975	0.924	Zero
F4	0.981	0.923	0.968	0.864	Zero
F5	0.992	0.838	0.976	0.877	Zero
F6	0.989	0.870	0.964	0.962	Zero
F7	0.983	0.907	0.973	0.821	Zero
F8	0.984	0.929	0.968	0.912	Zero

From the data and graphical representations, the Rosuvastatin nanoparticles formulations were showed well fitted zero order kinetics and formulation F1 was showed best among the formulations were prepared based on morphology, %drug loading efficiency, *in-vitro* drug released profiles and also well fitted the zero order kinetics.

Stability studies

FormulationF1was kept in room temperature**,** accelerated condition and refrigeratortemperature. After exposed to specified periods of time the samples were analyzed for %LE. Results were represented in Table 12.

Table 12: Stability studies of optimized formulation (F1).

S.No	Temperature(0^0c)	Drug loading efficiency(%LE)		
		1st month	2nd month	3rd month
1	25^0C±2^0C at RH 60%±5%	98.45	98.98	97.93
2	40^0C±2^0C at RH 75%±5%	98.55	96.80	96.92
3	5^0C±3^0C	98.29	98.14	97.35

No major difference was found between %LE before and after stability studies.Theformulation F1 was showed satisfactory physical stability at 25^0C ±2^0C at RH 60%±5%, 40^0C ±2^0C at RH 75%±5% and 5^0C±3^0C.

Zeta potential

The zeta potential report of the formulation F1 showed in Figure 8.33. The obtained valuewas the positive value.

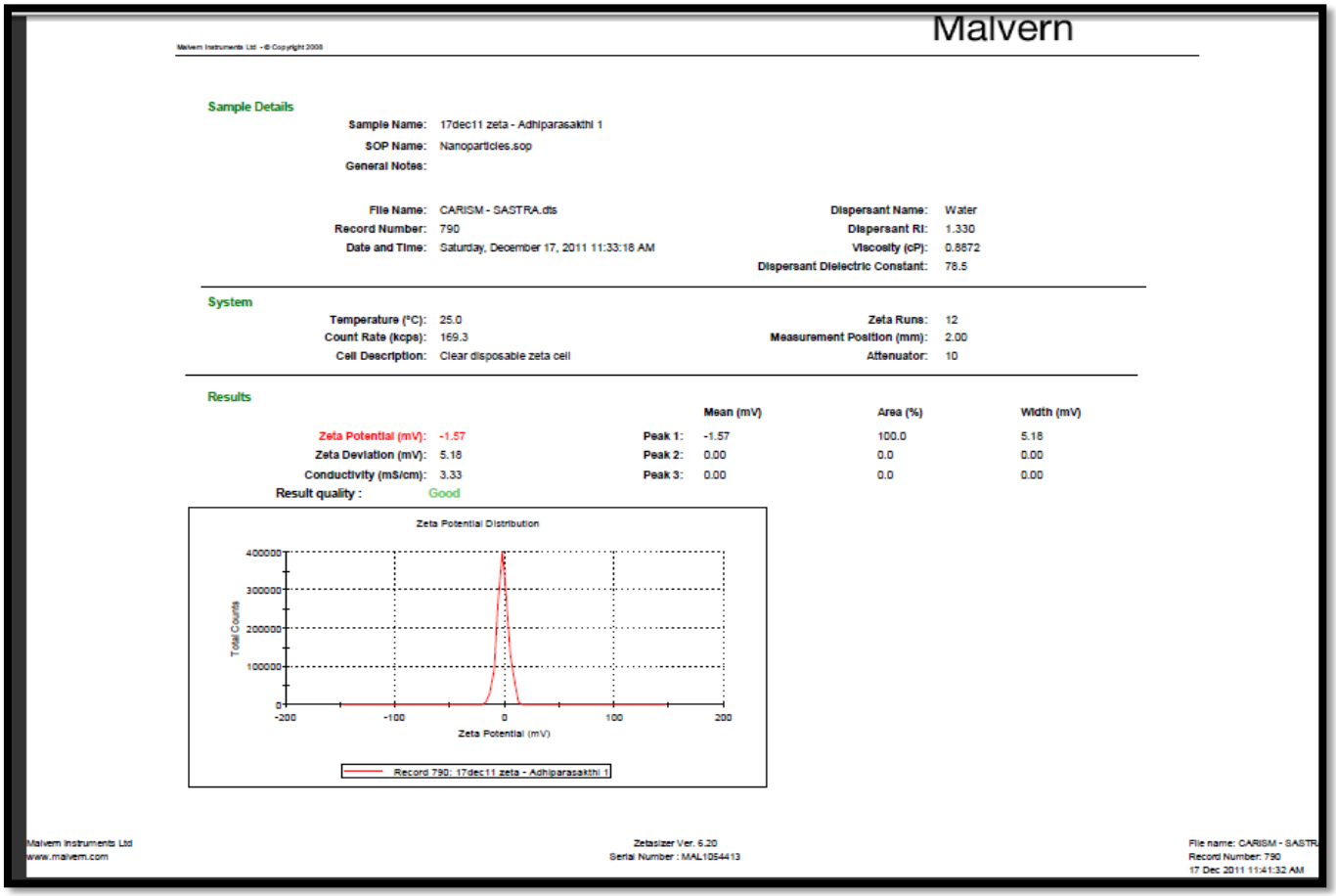

Figure 14: Zeta potential of F1 formulation

SUMMARY AND CONCLUSION:

The Rosuvastatin was widely used in the antilipidemic drug.This research work mainly focused on therapeutic effect of the drug to increased Bioavailability. The reported Bioavailability of Rosuvastatin was only 20%. While forming the novel drug delivery system in the form of nanoparticle to increased the bioavailability.

Eight formulations were prepared by using drug with gelatin A and gelatin B indifferent ratio of 1:1,1:2,1:3 and1:4 each polymer respectively(F1 to F8). Among the eight formulations F1 formulation was best because of these formulation shows the optimized result of colloidal drug delivery systems of nanoparticles have emerged as an efficient means enhancing the bioavailability with lowest possible dose.

The present work was proposed to prepared nanoparticles loaded with Rosuvastatin to achieved better bioavailability with low dose of the drug at the site, decreased the risk of adverse side effects. Rosuvastatin nanoparticles were prepared by *in-situ* two step desolvation method.

The loading efficiency(F1) and Entrapment efficiency(F1) was 66.21 and 91.73respectively.
The shape of nanoparticle was found to be spherical by SEM analysis. Formulation with high polymer content was observed to be fairly spherical. Compatibility of drug and polymer mixture was done by performing FTIR and DSC study. It was concluded that there was no interaction between drug and polymer.

The *in-vitro* released of Rosuvastatin was evaluated in phosphate buffer saline (pH6.8) up to 16hrs. The formulation F1 was released the drug 93.38% up to16 hours. and chosen the best among the formulations were prepared.

Zeta potential was determined for the formulation F1 and it was found to be +ve valueof 1.57mv.

The *in-vitro* drug released data was applied to various kinetic models like zero order kinetics, Higuchi plot, first order kinetics, and Peppas plot by predict the drug release kinetics mechanism. The formulation F1 was best fitted the zero order kinetics.

In short term stability studies the formulation F1 was showed that there was no remarkable changes in the % drug loading efficiency.

Based on the % drug loading efficiency, zeta potential, *in-vitro* drug release profile, *in-vitro* drug release kinetics and stability studies the formulation F1 was found to be best one among the formulations (F1 to F8) were prepared.

These nanoparticles can be promising agents for rational drug delivery in lipidemic condition.

REFERENCES:

1. Gaur M., Misra C., Yadav A.B., Swaroop S., Maolmhuaidh F., Bechelany M., Barhoum A. Biomedical Applications of Carbon Nanomaterials: Fullerenes, Quantum Dots, Nanotubes, Nanofibers, and Graphene. *Materials*. 2021;14:5978. doi: 10.3390/ma14205978. [PMC free article] [PubMed] [CrossRef] [Google Scholar]
2. Barhoum A., Pal K., Rahier H., Uludag H., Kim I.S., Bechelany M. Nanofibers as new-generation materials: From spinning and nano-spinning fabrication techniques to emerging applications. *Appl. Mater. Today*. 2019;17:1–35. doi: 10.1016/j.apmt.2019.06.015. [CrossRef] [Google Scholar]
3. Jeevanandam J., Barhoum A., Chan Y.S., Dufresne A., Danquah M.K. Review on nanoparticles and nanostructured materials: History, sources, toxicity and regulations. *Beilstein J. Nanotechnol.* 2018;9:1050–1074. doi: 10.3762/bjnano.9.98. [PMC free article] [PubMed] [CrossRef] [Google Scholar]
4. Barhoum A., El-Maghrabi H.H., Nada A.A., Sayegh S., Roualdes S., Renard A., Iatsunskyi I., Coy E., Bechelany M. Simultaneous hydrogen and oxygen evolution reactions using free-standing nitrogen-doped-carbon–Co/CoOx nanofiber electrodes decorated with palladium nanoparticles. *J. Mater. Chem. A.* 2021;9:17724–17739. doi: 10.1039/d1ta03704h. [CrossRef] [Google Scholar]
5. Prasad S., Kumar V., Kirubanandam S., Barhoum A. *Emerging Applications of Nanoparticles and Architecture Nanostructures: Current Prospects and Future Trends*. Elsevier Inc.; Amsterdam, The Netherlands: 2018. Engineered nanomaterials: Nanofabrication and surface functionalization; pp. 305–340. [CrossRef] [Google Scholar]
6. Cremers V., Rampelberg G., Barhoum A., Walters P., Claes N., de Oliveira T.M., Van Assche G., Bals S., Dendooven J., Detavernier C. Oxidation barrier of Cu and Fe powder by Atomic Layer Deposition. *Surf. Coat. Technol.* 2018;349:1032–1041. doi: 10.1016/j.surfcoat.2018.06.048. [CrossRef] [Google Scholar]
7. Hammani S., Moulai-Mostefa N., Samyn P., Bechelany M., Dufresne A., Barhoum A. Morphology, Rheology and Crystallization in Relation to the Viscosity Ratio of

Polystyrene/Polypropylene Polymer Blends. *Materials*. 2020;13:926. doi: 10.3390/ma13040926. [PMC free article] [PubMed] [CrossRef] [Google Scholar]
8. Barhoum A., Van Lokeren L., Rahier H., Dufresne A., Van Assche G. Roles of in situ surface modification in controlling the growth and crystallization of $CaCO_3$ nanoparticles, and their dispersion in polymeric materials. *J. Mater. Sci.* 2015;50:7908–7918. doi: 10.1007/s10853-015-9327-z. [CrossRef] [Google Scholar]
9. Rehan M., Barhoum A., Khattab T., Gätjen L., Wilken R. Colored, photocatalytic, antimicrobial and UV-protected viscose fibers decorated with Ag/Ag_2CO_3 and Ag/Ag_3PO_4 nanoparticles. *Cellulose*. 2019;26:5437–5453. doi: 10.1007/s10570-019-02497-8. [CrossRef] [Google Scholar]
10. Abdel-Haleem F.M., Salah A., Rizk M.S., Moustafa H., Bechelany M., Barhoum A. Carbon-based Nanosensors for Salicylate Determination in Pharmaceutical Preparations. *Electroanalysis*. 2019;31:778–789. doi: 10.1002/elan.201800728. [CrossRef] [Google Scholar]
11. Abdel-Haleem F., Mahmoud S., Abdel-Ghani N., El Nashar R., Bechelany M., Barhoum A. Polyvinyl Chloride Modified Carbon Paste Electrodes for Sensitive Determination of Levofloxacin Drug in Serum, Urine, and Pharmaceutical Formulations. *Sensors*. 2021;21:3150. doi: 10.3390/s21093150. [PMC free article] [PubMed] [CrossRef] [Google Scholar]
12. Abdel-Haleem F.M., Gamal E., Rizk M.S., Madbouly A., El Nashar R.M., Anis B., Elnabawy H.M., Khalil A.S.G., Barhoum A. Molecularly Imprinted Electrochemical Sensor-Based Fe_2O_3@MWCNTs for Ivabradine Drug Determination in Pharmaceutical Formulation, Serum, and Urine Samples. *Front. Bioeng. Biotechnol.* 2021;9:648704. doi: 10.3389/fbioe.2021.648704. [PMC free article] [PubMed] [CrossRef] [Google Scholar]
13. Parikha Mehrotra, Biosensors and their applications—A review. *J. Oral Biol. Craniofac. Res*. 2016;6:153–159. doi: 10.1016/j.jobcr.2015.12.002. [PMC free article] [PubMed] [CrossRef] [Google Scholar]
14. Rasouli R., Barhoum A., Uludag H. A review of nanostructured surfaces and materials for dental implants: Surface coating, patterning and functionalization for improved performance. *Biomater. Sci.* 2018;6:1312–1338. doi: 10.1039/C8BM00021B. [PubMed] [CrossRef] [Google Scholar]
15. Rasouli R., Barhoum A., Bechelany M., Dufresne A. Nanofibers for Biomedical and Healthcare Applications. *Macromol. Biosci.* 2018;19:e1800256. doi: 10.1002/mabi.201800256. [PubMed] [CrossRef] [Google Scholar]
16. Singh K.R., Nayak V., Singh J., Singh A.K., Singh R.P. Potentialities of bioinspired metal and metal oxide nanoparticles in biomedical sciences. *RSC Adv.* 2021;11:24722–24746. doi: 10.1039/D1RA04273D. [CrossRef] [Google Scholar]
17. Tan K.X., Barhoum A., Pan S., Danquah M.K. *Emerging Applications of Nanoparticles and Architecture Nanostructures: Current Prospects and Future Trends*. Elsevier Inc.; Amsterdam, The Netherlands: 2018. Risks and toxicity of nanoparticles and nanostructured materials; pp. 121–139. [CrossRef] [Google Scholar]
18. Kim D., Kim J., Park Y.I., Lee N., Hyeon T. Recent Development of Inorganic Nanoparticles for Biomedical Imaging. *ACS Central Sci.* 2018;4:324–336. doi: 10.1021/acscentsci.7b00574. [PMC free article] [PubMed] [CrossRef] [Google Scholar]
19. Mihai M.M., Dima M.B., Dima B., Holban A.M. Nanomaterials for Wound Healing and Infection Control. *Materials*. 2019;12:2176. doi: 10.3390/ma12132176. [PMC free article] [PubMed] [CrossRef] [Google Scholar]
20. Said M.M., Rehan M., El-Sheikh S.M., Zahran M.K., Abdel-Aziz M.S., Bechelany M., Barhoum A. Multifunctional Hydroxyapatite/Silver Nanoparticles/Cotton Gauze for Antimicrobial and Biomedical Applications. *Nanomaterials*. 2021;11:429. doi: 10.3390/nano11020429. [PMC free article] [PubMed] [CrossRef] [Google Scholar]
21. Kumar S., Bhushan P., Bhattacharya S. *Environmental, Chemical and Medical Sensors*. Springer; Berlin/Heidelberg, Germany: 2017. Fabrication of Nanostructures with Bottom-up Approach and Their Utility in Diagnostics, Therapeutics, and Others; pp. 167–198. [CrossRef] [Google Scholar]
22. Sawy A.M., Barhoumbb A., Gaber S.A.A., El-Hallouty S.M., Shousha W.G., Maarouf A.A., Khalilaf S.G.A. Insights of doxorubicin loaded graphene quantum dots: Synthesis, DFT drug interactions, and cytotoxicity. *Mater. Sci. Eng. C*. 2021;122:111921. doi: 10.1016/j.msec.2021.111921. [PubMed] [CrossRef] [Google Scholar]